Optimization of GaAs Solar Cell Performance and Growth Efficiency at MOVPE Growth Rates of 100 µm/h

Robin Lang, Jonas Schön, Frank Dimroth, *Member, IEEE*, and David Lackner

***Abstract*— III-V devices outperform all other solar cells in terms of efficiency. However, the manufacturing of these cells is expensive and prevents their use in a number of applications which would benefit from the high efficiency. A major contribution to the cost is the metal-organic-vapor-phase epitaxy process for the III-V compounds. Increasing growth rates, and hence machine throughput, as well as the growth efficiency are important steps towards reducing the cost of III-V solar cells. We demonstrate the growth of GaAs solar cells at extremely high growth rates of 100 µm/h and achieve a V_{OC} of 1.028 V, a base diffusion length of 6.5 µm and an efficiency of 23.6 % under AM1.5g conditions. Furthermore, we show reactor adjustments leading to growth rates up to 140 µm/h and reach conditions where more than half of the Ga from the precursor is incorporated into the solar cell layers. The results are encouraging and demonstrate a pathway towards lower cost III-V solar cell manufacturing.**

***Index Terms*—III-V semiconductor materials, gallium arsenide, high growth rates, MOVPE, OMVPE, solar cells**

I. Introduction

The current world record conversion efficiencies of 46.1 % for a 4-junction cell at 312 suns [1] and of 28.8 % for a single-junction cell under AM1.5g illumination [2] are held by III-V solar cells. Although they exhibit the highest efficiencies, their high cost still limits their use to space applications and concentrator photovoltaics.

The cost for III-V epitaxy needs to be decreased significantly for it to be an economic alternative for applications like terrestrial flat panels. One component of the cost reduction is the development of ultrafast epitaxy processes with efficient use of the precursors. At the same time, a high material quality must be maintained.

Recent findings by Schmieder et al. show promising results in this direction [3]. A gallium arsenide (GaAs) solar cell grown at 60 µm/h achieved a V_{OC} of 1.011 V and an efficiency of 23.8 %, only 0.8 $\%_{abs}$ below the reference cell grown at 14 µm/h. The paper also suggests the EL2 defect as a possible cause for this decrease.

Another group has grown GaAs solar cells at 80 µm/h with an n-doped base layer and no difference from a reference cell grown at 20 µm/h [4].

In this work, we present growth conditions that lead to GaAs growth rates up to 140 µm/h and simultaneously increase the growth efficiency for group III molecules. The material quality and homogeneity is investigated through diffusion length measurements as well as other measurements. These investigations are followed by solar cell results for growth rates up to 100 µm/h.

II. Experimental Methods

All samples were grown by metal-organic-vapor-phase epitaxy (MOVPE) in an Aixtron CRIUS Close Coupled Showerhead (CSS) reactor in a 7x4“ susceptor configuration operated at 100 mbar. This reactor has a very short, adjustable gas mixing distance between the gas inlet and the substrates. The substrates are 4” GaAs (100) wafers with 6° offcut towards the <111>B direction. The precursors and gases used were trimethylgallium (TMGa), trimethylindium (TMIn), trimethylaluminium (TMAl), arsine (AsH_3), phosphine (PH_3), silane (SiH_4) and dimethylzinc (DMZn). The growth temperature was between 640 °C and 770 °C, and the V/III ratio for the GaAs layers was varied between 3 and 13, while the reactor pressure was kept constant at 100 mbar. The growth temperature was measured directly on the wafer surface using a pyrometer and a wavelength of 950 nm. Growth rate, doping concentration, surface roughness and morphology were determined using high resolution x-ray diffraction (HR-XRD), electrochemical capacitance-voltage (ECV), and atomic force microscopy (AFM) measurements, respectively. The AFM and HR-XRD measurements were performed on a 400 nm GaAs grown on top of a 50 nm AlGaAs layer.

Cathodoluminescence (CL) measurements were performed to quantify the diffusion length using a Gatan CL-Setup in a Hitachi SU-70 scanning electron microscope. Diffusion length measurements were performed using the CL signal decay perpendicular to a metal edge on top of p-doped GaAs double-hetero (DH) structures (see Fig. 1A). Further details concerning the method can be found in [5].

Manuscript received June 7, 2018. (*Corresponding author: Robin Lang*.) This work was supported by the German Federal Ministry of Education and Research under Grant “MehrSi” 03SF0525A.

R. Lang, J. Schön, F. Dimroth, and D. Lackner are with the Fraunhofer Institute for Solar Energy Systems, ISE, Freiburg 79110, Germany (e-mail: robin.lang@ise.fraunhofer.de, jonas.schoen@ise.fraunhofer.de, frank.dimroth@ise.fraunhofer.de, david.lackner@ise.fraunhofer.de).

In this structure, the p-GaAs target layer (red) is sandwiched between two barriers to avoid interface recombination. A strain balanced multi-quantum well layer stack is incorporated between the semi-insulating substrate and the target layer to prevent any photon coupling between them. This ensures that only the target layer bulk diffusion length is measured. The growth rate and V/III ratio variations were applied only to the target layer, whereas the growth temperature was kept constant for the whole DH structure.

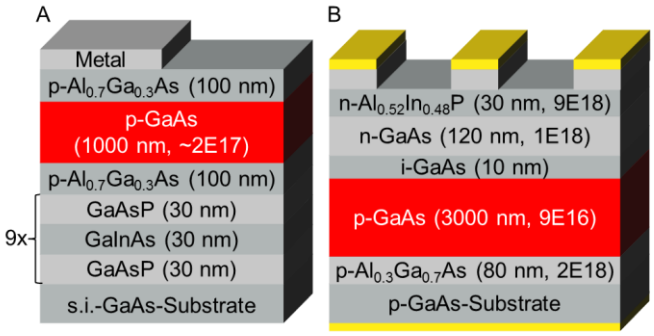

Fig. 1. A) DH structures grown for CL-measurements to quantify the diffusion length. Conditions were only varied for the p-GaAs target layer (red). B) Structure of the solar cells grown within this work. Only the p-GaAs base layer (red) was grown at different conditions. There is a 400 nm highly n-doped GaAs layer below the top contacts.

GaAs solar cells were investigated under different growth conditions (see Fig. 1B). The growth rate and V/III ratio variation were varied in the base layer only. The growth time for this layer drops from 45 minutes to less than 2 minutes when the growth rate is increased from 4 to 100 µm/h. The growth temperature was changed from the standard process for the whole structure except for the last two layers. Window and cap layer were always grown at 640 °C. For some of the solar cells, a dual-layer anti-reflection coating (ARC) consisting of Ta_2O_5/MgF_2 was applied. All of the solar cells were processed in the cleanroom at Fraunhofer ISE and measured under the AM1.5g spectrum using a LOANA measurement system.

III. Results And Discussion

A. *High Growth Rates*

In the first step, the expected linear relationship between the growth rate and the TMGa flow was investigated for growth rates up to 100 µm/h. From the results shown in Fig. 2, it is evident that this linear relation is not fulfilled at a growth temperature of 640 °C if the growth rate exceeds 60 µm/h. The measurement points at 80 and 100 µm/h clearly deviate from the dashed line, which represents a linear fit through the origin and the measurements up to 60 µm/h.

This effect can be compensated by going to higher growth temperatures; growths at 720 °C and 770 °C show a linear dependence for the whole investigated range of molecular flows. Therefore, neither parasitic absorption on the reactor walls nor vapor pressure saturation is the cause for the non-linear behavior. Thus it has to be a kinetic limitation, however TMGa is already fully decomposed at 640 °C, and since there is no significant difference in the growth rate between 720 °C and 770 °C, we are in the mass flow limited regime. If the surface diffusion would be limiting the growth, we would expect a roughening of the surface, but AFM measurements for all of the samples from Fig. 2 show neither a difference in surface morphology, nor a significant change in surface roughness (see Fig. 3). The root mean square (RMS) value was below 0.3 nm for all measured samples. Representative measurements for 30 and 100 µm/h are shown in Fig. 3A and B, respectively. We therefore assume a kinetic limitation in the diffusion towards or through the boundary layer due to the high TMGa flows above 8 µmol/min.

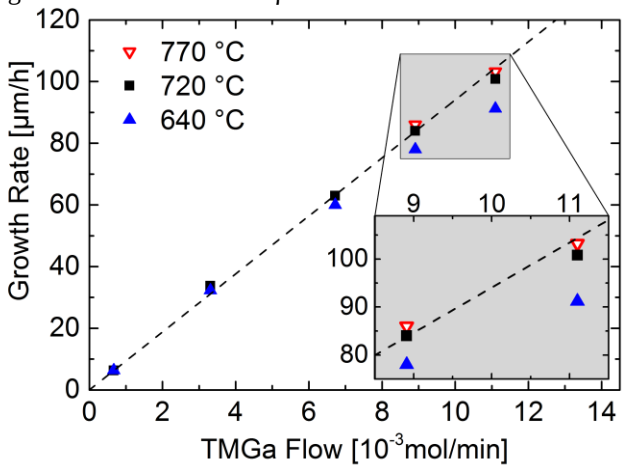

Fig. 2. Growth rate (determined by HR-XRD) plotted versus the TMGa flow into the reactor for different growth temperatures. The dashed line represents a linear fit using the origin and the measurements up to 60 µm/h. The V/III ratio for all the layers was 10.

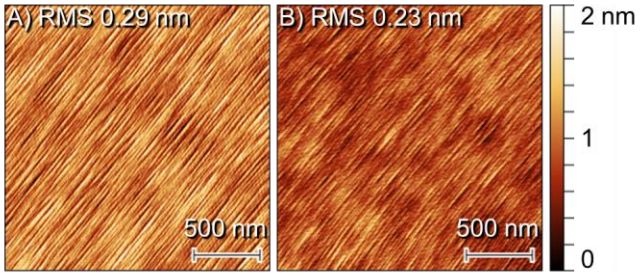

Fig. 3. Representative AFM measurements of 400 nm GaAs grown at a growth rate of A) 30 µm/h and B) 100 µm/h. The GaAs layers were grown at 720 °C and with a V/III ratio of 10.

The efficiency of the Ga incorporation can be calculated from the linear fit between growth rate and TMGa flow in Fig. 2. For 7 wafers in the 7x4" susceptor configuration that was used in this work, this translates into a group III growth efficiency of about 30 %. The gas mixing distance between gas inlet and substrates in the CRIUS reactor can be adjusted from 7 to 16 mm. The driving force for the atoms towards the substrate surface arises from the concentration gradient within this gap [6, pp. 74-75], which can be increased in one of two ways. Either the gap distance can be decreased or the total carrier gas flow can be lowered in order to increase the partial pressure of the material. The results from both experiments are shown in Fig. 4. All samples were grown with the same TMGa flow at 720 °C growth temperature and with a V/III ratio of

10.

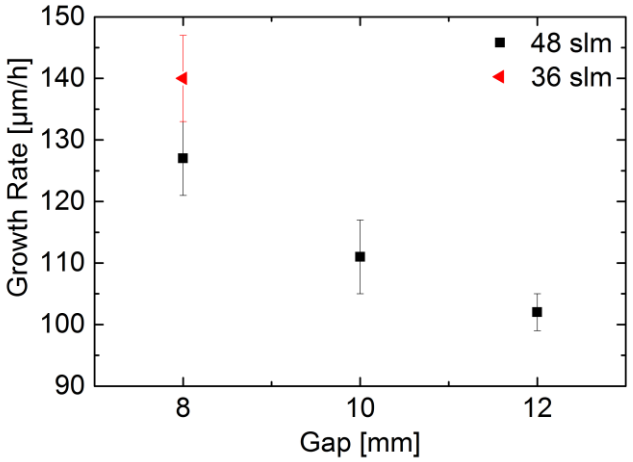

Fig. 4. Growth rate (determined by HR-XRD) plotted versus reactor gap for different total carrier gas flows of 36 and 48 slm. The gap denotes the distance between gas inlet and substrates and the TMGa flow was constant for all samples. The GaAs layers were 400 nm thick and grown at 720 °C and with a V/III ratio of 10.

Reducing the gap from 12 to 8 mm led to an increase of 25 % in the growth rate. When the total carrier gas flow was simultaneously reduced by one quarter from 48 to 36 slm, it led to a further increase of 11 %. In total, the growth rate could be increased by 40 % through these reactor adjustments. This resulted in a peak growth rate for GaAs of 140 µm/h. Such high growth rates are usually only known for liquid phase epitaxy (LPE) and hydride vapor phase epitaxy (HVPE) [7, 8]. Assuming the use of one 300 mm diameter wafer, 55 % of the Ga would be incorporated into the GaAs film. This is a very high efficiency for the use of the precursor molecules.

Higher growth rates are only useful for device fabrication if sufficient homogeneity across the wafer can be achieved. In the showerhead design of the CRIUS reactor, the susceptor rotates with fixed substrates. We measured the growth rate on several spots perpendicular to the susceptor rotation for all of the samples from Fig. 4 and a reference GaAs sample grown with 4 µm/h. There was no directional trend observed in the results, and the growth rates measured were all well within the error bars shown in Fig. 4.

B. Material Quality

The diffusion length for GaAs growth rates between 4 µm/h and 100 µm/h was investigated as shown in Fig. 5A. Here, it is found that the diffusion length drops from around 12 µm to less than 3 µm, when the growth rate is increased 25 times from 4 µm/h to 100 µm/h. Increasing the growth temperature to 720 °C doubles the diffusion length, but a further increase to 740 °C shows no effect.

Schmieder et al. have seen a similar trend for high growth rates [3]. They investigated n-GaAs DLTS structures grown at 640 °C with different growth rates and saw a strong increase in trap density for higher rates. The main defect in these structures was identified as the EL2 complex, which is connected to an As antisite (As_{Ga}). It was possible to reduce the trap density considerably by increasing the growth temperature to 680 °C, explained by an increased adatom surface mobility and thus reduced defect formation at higher growth temperatures [3]. The As antisite defect density is expected to reduce with the arsenic excess during growth [9]. Therefore, a lower V/III ratio should have a positive effect on the trap density and subsequently the diffusion length.

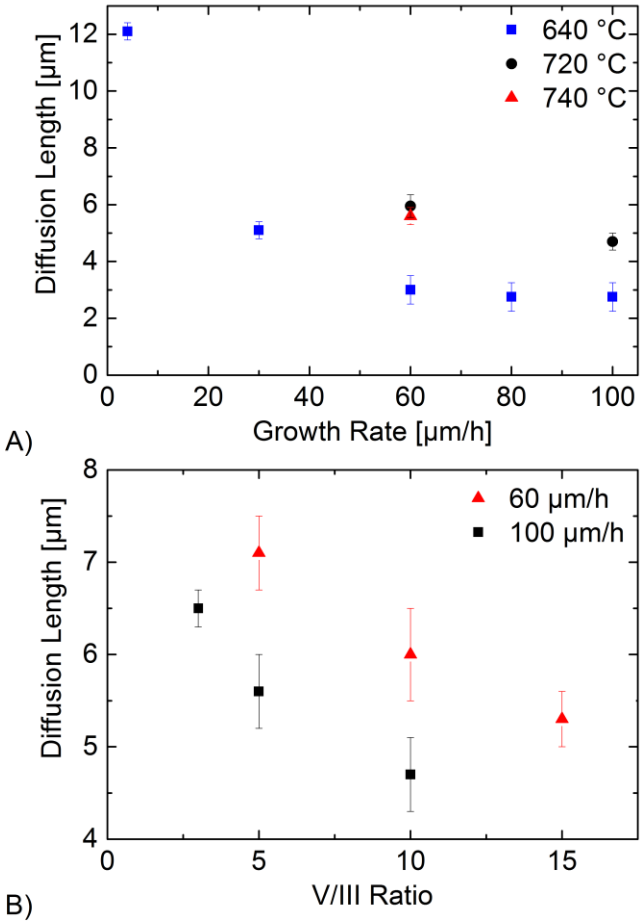

Fig. 5. a) Diffusion length plotted versus growth rate for different growth temperatures and a constant V/III ratio of 10. b) Diffusion length plotted versus V/III ratio for different growth rates at a growth temperature of 720 °C. The measured DH structure is displayed in Fig. 1.

Three DH structures were grown with varying V/III ratio at 60 and 100 µm/h respectively (see Fig. 5B). It was found that a lower V/III ratio is beneficial and the diffusion length increases from 5.3 to over 7 µm if the V/III ratio is decreased from 15 to 5 at a growth rate of 60 µm/h. At 100 µm/h, the diffusion length increases from 4.6 to 6.5 µm if the V/III ratio is decreased from 10 to 3. With these results, two sets of solar cells were designed for high growth rates.

C. Solar Cell Results

TABLE I
AM1.5G BEST 4 CM² CELL RESULTS (WITH ARC)

Growth Rate µm/h	T_g °C	V/III ratio	V_{OC} V	J_{SC} mA/cm²	FF %	η %
4	640	13	1.055	28.6	81.6	24.6
60	720	5	1.036	28.4	79.7	23.5
80	720	5	1.021	28.3	80.9	23.4
100	720	5	1.019	28.3	81.1	23.3

The first set of GaAs solar cells to test the influence of the growth rate is displayed in Table I. The reference GaAs solar cell was grown at a growth temperature of 640 °C with a growth rate of 4 µm/h and a V/III ratio of 13. The growth rates were then increased to 100 µm/h, and a temperature of 720 °C with a V/III ratio of 5 was chosen.

The results of the growth rate variation are summarized in Table I. The light IV parameters are shown for the best 4 cm² solar cells with an ARC and under AM1.5g illumination. The open-circuit voltage (V_{OC}) decreases as the growth rate is increased. At 100 µm/h, the V_{OC} is 1019 mV, which is 36 mV lower than the reference cell with a V_{OC} of 1055 mV. The short-circuit current density (J_{SC}) remains constant, while the fill factor (FF) varies between 79.7 and 81.6 %. The efficiency drops by 1.3 $\%_{abs}$ when the growth rate is increased to 100 µm/h. Overall, these are encouraging results for a GaAs solar cell on substrate.

Numerical device modeling of these solar cells allows for more detailed analysis of losses. The modeling was performed using TCAD Sentaurus [10], which is a commercial software package that has previously been used to model GaAs single and dual-junction solar cells to sufficiently high accuracy [11–13]. The material parameters for GaAs are reported in [11]. The non-radiative recombination lifetime is the central parameter for a simultaneous fitting of measured IQE, dark IV, and V_{OC}. Additionally, a lumped series resistance is used for the dark IV fit at high voltages. The electron diffusion length in the base layer is determined by calculating the radiative lifetime and fitting the V_{OC} and EQE simultaneously by adjusting the non-radiative lifetime.

Only the solar cells with lowest (4 µm/h) and highest (100 µm/h) growth rate were simulated with Sentaurus to analyze the difference in material quality. For the cells with low growth rate, a good agreement with measured IQE, light and dark IV was found for a non-radiative recombination lifetime of 100 ns in the base. An even better fit of simulated and measured dark IV can be achieved if the non-radiative recombination lifetime in the space charge region and the emitter is reduced to 40 ns (see Fig. 7). The lower lifetime in the space charge region reflects the high J_{02} extracted from the dark IV measurement. We account for the recombination at the window/emitter and the window/ARC interface with a surface recombination velocity of $1x10^6$ cm/s and $3x10^6$ cm/s respectively. Recombination at the other interfaces seems to be negligible.

The measurements of the fast grown sample (100 µm/h) can be reproduced well by assuming an additional defect in the base. This additional defect in the fast grown sample reduces the non-radiative electron lifetime in the base to 4 ns thereby reducing the V_{OC} of this cell to 1019 mV. The majority charge carrier (hole) lifetime is barely affected. The p-type GaAs lifetime from the simulation corresponds to a diffusion length of 16 µm for the reference cell (measured 12.2 µm) and of 6 µm for the fast grown sample (measured 5.6 µm); both values are corrected for the different doping concentrations in the DH structures and the solar cells solely by changing the radiative lifetime. Some of the discrepancy between simulation and measurement might be explained by the assumption of a constant non-radiative lifetime which is not true for different doping levels in p-type material [14] or by additional surface recombination in the DH structures.

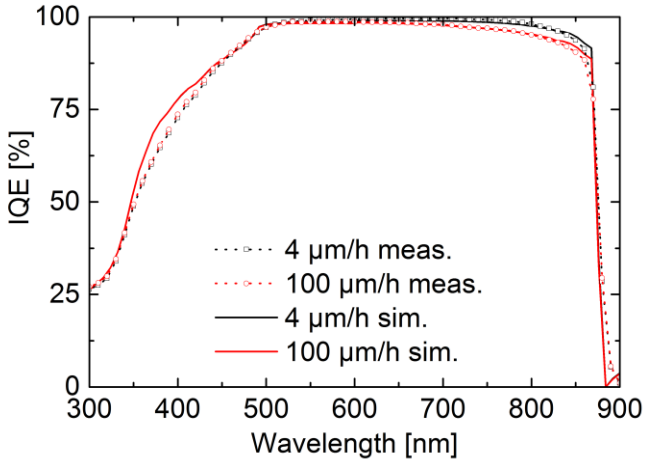

Fig. 6. EQE of the best GaAs solar cells grown at 4 and 100 µm/h from Table I. The markers represent the measured data and the lines represent the simulations conducted with TCAD Sentaurus.

A comparison of the IQE measurements and simulations is shown in Fig. 6. The lines represent the simulated IQE curves and fit very well to the measured data. The modelled V_{OC} is 1046 mV for the cell grown at 4 µm/h (9 mV below the measurement) and 1006 mV for the cell grown at 100 µm/h (13 mV below measurement). The simulated V_{OC} difference of 40 mV between these two cells agrees well with the measured difference of 36 mV (see Table I). Therefore, the difference in solar cell performance at different growth rates can be attributed to the difference in base layer lifetime.

All solar cells exhibit a low FF with no discernible trend in regard to growth rate, so it is not connected to the increasing growth rate. Additionally, FFs of around 86 % have already been shown for high growth rate GaAs cells [3]. SunsV_{OC} measurements were performed to determine if the low FF in our experiments is due to a limitation of series resistance (R_S) or of saturation current density (J_{02}). A pseudo FF (effect of R_S excluded) of 84 % was measured, indicating a limitation by both, R_S and J_{02}.

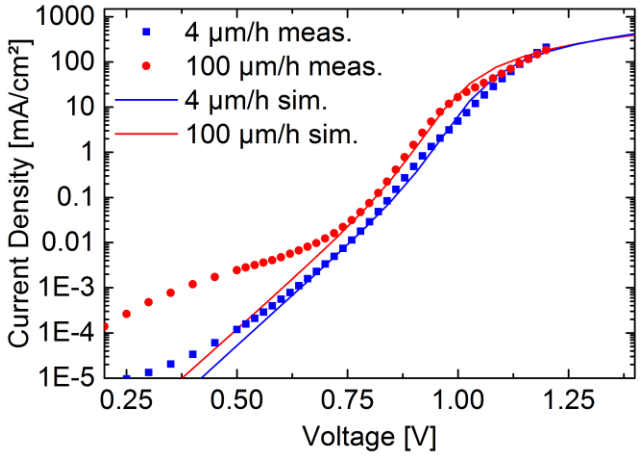

Fig. 7. Dark IV curves of the best GaAs solar cells grown at 4 and 100 µm/h from Table I. The markers represent the measured data and the lines represent the simulations conducted with TCAD Sentaurus.

This is in agreement with the simulations. Dark IV measurements for the solar cells grown at 4 µm/h and 100 µm/h and their respective simulations are shown in Fig. 7. A high series resistance (R_S) of about 700 mΩ·cm² must be assumed for a good match between simulation and measurement. The dark IV curves also show a high J_{02}, that contributes about 1.5 $\%_{abs}$ in FF losses. The reason for the unexpectedly high R_S and the J_{02} values are currently under investigation.

TABLE II
AM1.5G BEST 4 CM² CELL RESULTS (WITHOUT ARC)

Growth Rate µm/h	T_g °C	V/III ratio	V_{OC} V	J_{SC} mA/cm²	FF %	η %
60	720	10	1.005	22.0	83.3	18.4
60	720	5	1.026	22.2	82.1	18.7
60	720	3	1.004	22.0	74.8	16.5

The second set of solar cells contains a variation of the V/III ratio at growth rates of 60 µm/h (without ARC) and 100 µm/h (with ARC) shown in Tables II and III. The growth temperature was kept at 720 °C. At 60 µm/h the cell with a ratio of 5 has a 21 mV higher V_{OC} and slightly higher J_{SC} compared to the one with a ratio of 10. This matches the previous results from the diffusion length measurements. A further decrease to 3 does not improve the quality further; rather, this solar cell is even worse than the one grown with a ratio of 10.

TABLE III
AM1.5G BEST 4 CM² CELL RESULTS (WITH ARC)

Growth Rate µm/h	T_g °C	V/III ratio	V_{OC} V	J_{SC} mA/cm²	FF %	η %
100	720	5	1.019	28.3	81.1	23.3
100	720	3	1.028	28.5	80.7	23.6

At 100 µm/h the decrease in V/III ratio from 5 to 3 still leads to an improvement in solar cell performance, matching the diffusion length results. The V_{OC} increases by 9 mV and the efficiency by 0.3 $\%_{abs}$.

The most likely explanation for the different behavior at different growth rates is desorption of arsenic. It was observed with regard to zinc doping that at higher temperatures, the Zn incorporation is decreased. This was expected, as zinc is known to desorb from the surface [15]. However the zinc incorporation increases with growth rate. The dependency of arsenic desorption is expected to be the same. Desorption is enhanced at higher growth temperatures, reducing the effective V/III ratio on the substrate surface. This effective ratio depends on how much time the system has to desorb and this time can be reduced by increasing the growth rates. Therefore, higher growth rates allow for lower input V/III ratios.

IV. CONCLUSION

We have presented GaAs single-junction cells grown at 100 µm/h, reaching a V_{OC} of 1.028 V and an efficiency of 23.6 % under the AM1.5g spectrum. This is only 1.0 $\%_{abs}$ below a reference structure grown at 4 µm/h. The diffusion length is found to decrease with increasing growth rate, and this is attributed to a higher density of As antisite defects which can be partly suppressed by lowering the V/III ratio.

Growth rates up to 140 µm/h were presented with a very efficient group III incorporation. This was achieved through reactor adjustments that led to a higher concentration gradient between gas inlet and substrate within the reactor. More than 50% of the Ga which is introduced into the reactor can be incorporated into the layer, and the growth rate homogeneity over the wafer did not degrade at these high growth rates. The results are encouraging towards reaching lower cost GaAs epitaxy through optimization of growth conditions, and they show the potential of using metal-organic-vapor-phase epitaxy, which is the established technology for III-V solar cell manufacturing.

ACKNOWLEDGMENT

The authors would like to thank the technology group for the processing of the solar cells, Elisabeth Schäffer and Felix Martin for the solar cell measurements and Sophie Stättner and Markus Feifel for help with the MOVPE machine.

REFERENCES

[1] F. Dimroth, T. N. D. Tibbits, M. Niemeyer, F. Predan, P. Beutel, C. Karcher, E. Oliva, G. Siefer, D. Lackner, P. Fus-Kailuweit, A. W. Bett, R. Krause, C. Drazek, E. Guiot, J. Wasselin, A. Tauzin, and T. Signamarcheix, "Four-Junction Wafer-Bonded Concentrator Solar Cells," *IEEE J. Photovolt.*, vol. 6, no. 1, pp. 343–349, 2016.

[2] B. M. Kayes, H. Nie, R. Twist, S. G. Spruytte, F. Reinhardt, I. C. Kizilyalli, and G. S. Higashi, "27.6% Conversion efficiency, a new record for single-junction solar cells under 1 sun illumination," in *2011 37th IEEE Photovoltaic Specialists Conference*, Seattle, WA, USA, 2011, pp. 4–8.

[3] K. J. Schmieder, E. A. Armour, M. P. Lumb, M. K. Yakes, Z. Pulwin, J. Frantz, and R. J. Walters, "Effect of Growth Temperature on GaAs Solar Cells at High MOCVD Growth Rates," *IEEE J. Photovoltaics*, vol. 7, no. 1, pp. 340–346, 2017.
[4] A. Ubukata, H. Sodabanlu, K. Watanabe, S. Koseki, Y. Yano, T. Tabuchi, T. Sugaya, K. Matsumoto, Y. Nakano, and M. Sugiyama, "Accelerated GaAs growth through MOVPE for low-cost PV applications," *J. Cryst. Growth*, vol. 489, pp. 63–67, 2018.
[5] H. A. Zarem, P. C. Sercel, J. A. Lebens, L. E. Eng, A. Yariv, and K. J. Vahala, "Direct determination of the ambipolar diffusion length in GaAs/AlGaAs heterostructures by cathodoluminescence," *Appl. Phys. Lett.*, vol. 55, no. 16, pp. 1647–1649, 1989.
[6] G. B. Stringfellow, *Organometallic Vapor-Phase Epitaxy: Theory and Practice*, 2nd ed. San Diego, USA: Academic Press, 1999.
[7] K. Grüter, M. Deschler, H. Jürgensen, R. Beccard, and P. Balk, "Deposition of high quality GaAs films at fast rates in the LP-CVD system," *Journal of Crystal Growth*, vol. 94, no. 3, pp. 607–612, 1989.
[8] V. Tassev, D. Bliss, C. Lynch, C. Yapp, W. Goodhue, and K. Termkoa, "Low pressure–temperature–gas flow HVPE growth of GaP for nonlinear optical frequency conversion devices," *Journal of Crystal Growth*, vol. 312, no. 8, pp. 1146–1149, 2010.
[9] L. Samuelson, P.O.'H. Titze, and H. G. Grimmeiss, "Electrical and optical properties of deep levels in MOVPE grown GaAs," *Journal of Crystal Growth*, vol. 55, no. 1, pp. 164–172, 1981.
[10] Synopsys, "Sentaurus TCAD," 2010.
[11] A. W. Walker, O. Hohn, D. N. Micha, B. Bläsi, A. W. Bett, and F. Dimroth, "Impact of Photon Recycling on GaAs Solar Cell Designs," *IEEE J. Photovolt.*, vol. 5, no. 6, pp. 1636–1645, 2015.
[12] G. Létay, M. Hermle, and A. W. Bett, "Simulating Single-junction GaAs Solar Cells Including Photon Recycling," *Prog. Photovolt., Res. Appl.*, vol. 14, no. 8, pp. 683–696, 2006.
[13] M. Hermle, G. Létay, B. Mack, and A. W. Bett, "Simulation of Single Junction GaAs Solar Cells Considering Optical Coupling," in *Proceedings of the 20th European Photovoltaic Solar Energy Conference*, Barcelona, Spain, 2005, pp. 511–514.
[14] M. P. Lumb, M. A. Steiner, J. F. Geisz, and R. J. Walters, "Incorporating photon recycling into the analytical drift-diffusion model of high efficiency solar cells," *Journal of Applied Physics*, vol. 116, no. 19, p. 194504, 2014.
[15] R. W. Glew, "Zinc Doping of MOCVD GaAs," *Journal of Crystal Growth*, vol. 68, no. 1, pp. 44–47, 1984.